CHEMISTRY
A EUROPEAN JOURNAL

DOI: 10.1002/chem.200500885

Nucleic Acid Intercalators and Avidin Probes Derived from Luminescent Cyclometalated Iridium(III)–Dipyridoquinoxaline and –Dipyridophenazine Complexes

Kenneth Kam-Wing Lo,*[a] Chi-Keung Chung,[a] and Nianyong Zhu[b]

Abstract: Six luminescent cyclometalated iridium(III)–dipyridoquinoxaline and –dipyridophenazine complexes $[Ir(ppy)_2(N\text{-}N)](PF_6)$ (Hppy = 2-phenylpyridine; N-N = dipyrido[3,2-*f*:2′,3′-*h*]quinoxaline, dpq (**1**); 2-*n*-butylamidodipyrido[3,2-*f*:2′,3′-*h*]quinoxaline, dpqa (**2**); 2-((2-biotinamido)ethyl)amidodipyrido[3,2-*f*:2′,3′-*h*]quinoxaline, dpqB (**3**); dipyrido[3,2-*a*:2′,3′-*c*]phenazine, dppz (**4**); benzo[*i*]dipyrido[3,2-*a*:2′,3′-*c*]phenazine, dppn (**5**); 11-((2-biotinamido)ethyl)amidodipyrido[3,2-*a*:2′,3′-*c*]-phenazine, dppzB (**6**)) have been designed as luminescent intercalators for DNA and probes for avidin. The structure of complex **4** has been studied by X-ray crystallography. The photophysical and electrochemical properties of the complexes have also been investigated. The binding of these complexes to double-stranded calf thymus DNA and synthetic double-stranded oligonucleotides poly(dA)·poly(dT) and poly(dG)·poly(dC) has been investigated by spectroscopic titrations. The interactions between the two biotin-containing complexes and avidin have been studied by 4′-hydroxyazobenzene-2-carboxylic acid (HABA) assays and emission titrations.

Keywords: avidin · biotin · DNA · iridium · luminescence

Introduction

Interactions between transition-metal complexes and nucleic acid molecules continue to receive much attention.[1] In particular, complexes containing intercalating ligands such as dipyrido[3,2-*f*:2′,3′-*h*]quinoxaline (dpq) and dipyrido[3,2-*a*:2′,3′-*c*]phenazine (dppz) have been the focus of many studies.[2–13] Whilst transition-metal centers such as ruthenium(II),[2,3,4a–d,g,5,6,8b,13b] osmium(II),[4e] rhenium(I),[7,8a,9,10] rhodium(III),[13a] chromium(III),[11] cobalt(III),[12] and nickel(II)[12] have been extensively studied, related probes derived from iridium(III) have been relatively unexplored.[4f,13a,14] Examples include the redox-active complex $[Ir(bpy)(phen)(phi)]^{3+}$ (bpy = 2,2′-bipyridine; phen = 1,10-phenanthroline; phi = 9,10-phenanthrenequinonediimine) that has been employed to study electron transfer in DNA molecules.[4f] The DNA-binding properties of the organometallic iridium(III) complexes $[(\eta^5\text{-}C_5Me_5)Ir(Aa)(dppz)]^{n+}$ (Aa = (*S*)-amino acids) have been studied by absorption titrations, NMR spectroscopy, and gel electrophoresis.[13a] Recently, an iridium(III)–dppz complex has also been included as a member of a combinatorial library.[14] Despite these reports, the design of DNA probes derived from luminescent iridium(III) complexes has not been investigated.

In view of the interesting photophysical and photochemical properties of luminescent iridium(III)–polypyridine complexes[15–30] and our recent interest in using these complexes as biological labels and probes,[30] we anticipate that they can be exploited as new luminescent intercalators for DNA molecules and probes for proteins. We report here the synthesis, photophysical, and electrochemical properties of six luminescent cyclometalated iridium(III) complexes containing an extended planar diimine ligand, $[Ir(ppy)_2(N\text{-}N)](PF_6)$ (Hppy = 2-phenylpyridine; N-N = dipyrido[3,2-*f*:2′,3′-*h*]quinoxaline, dpq (**1**); 2-*n*-butylamidodipyrido[3,2-*f*:2′,3′-*h*]quinoxaline, dpqa (**2**); 2-((2-biotinamido)ethyl)amidodipyrido[3,2-*f*:2′,3′-*h*]quinoxaline, dpqB (**3**); dipyrido[3,2-*a*:2′,3′-*c*]phenazine, dppz (**4**); benzo[*i*]dipyrido[3,2-*a*:2′,3′-*c*]phenazine, dppn (**5**); 11-((2-biotinamido)ethyl)amidodipyrido[3,2-*a*:2′,3′-*c*]phenazine, dppzB (**6**)) (see below). The structure of complex **4** has been studied by X-ray crystallography. The binding of the complexes to double-stranded calf thymus

[a] Dr. K. K.-W. Lo, C.-K. Chung
Department of Biology and Chemistry
City University of Hong Kong
Tat Chee Avenue, Kowloon, Hong Kong
People's Republic of China
Fax: (+852) 2788-7406
E-mail: bhkenlo@cityu.edu.hk

[b] Dr. N. Zhu
Department of Chemistry, The University of Hong Kong
Pokfulam Road, Hong Kong
People's Republic of China

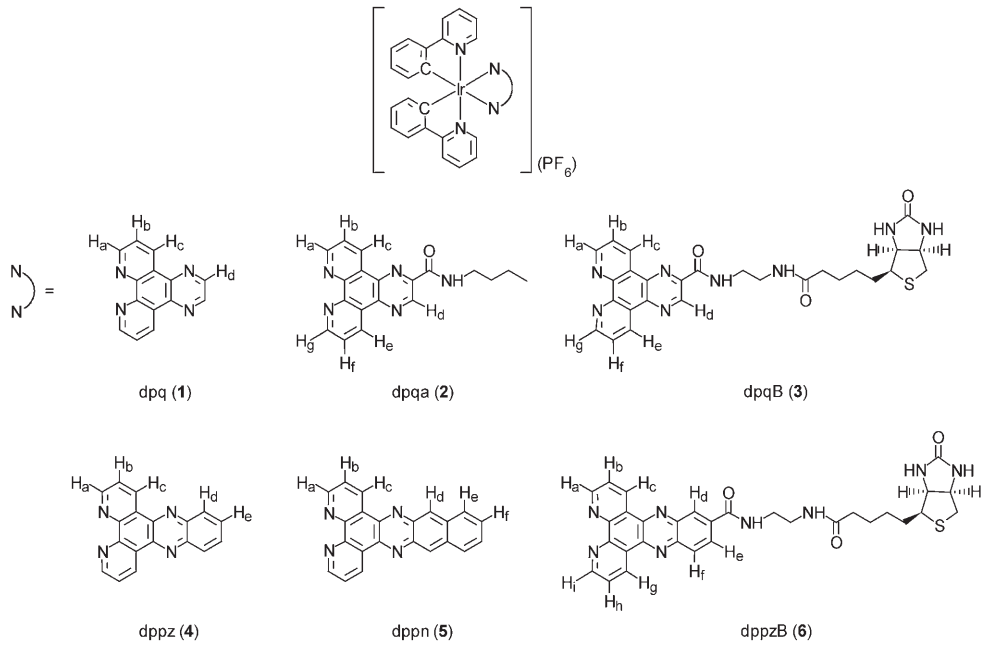

DNA and synthetic double-stranded oligonucleotides poly(dA)·poly(dT) and poly(dG)·poly(dC) has been investigated by spectroscopic titrations. The interactions between the biotin-containing complexes and avidin have been studied by 4′-hydroxyazobenzene-2-carboxylic acid (HABA) assays and emission titrations.

Results and Discussion

Synthesis: The ligands dpq,[2b] dpqa,[31] dppz,[32] and dppn[32] were synthesized according to reported procedures. The biotin-containing ligands dpqB and dppzB were prepared by using two different approaches. The ligand dpqB was obtained from the reaction of 2-((2-amino)ethyl)amidodipyrido[3,2-*f*:2′,3′-*h*]quinoxaline (dpq-en) with biotinyl-*N*-hydroxysuccinimidyl ester (biotin-NHS)[33] in DMF at 60 °C. The ligand dppzB was obtained from the reaction of 1,1-carbonyldiimidazole (CDI)-activated dipyrido[3,2-*a*:2′,3′-*c*]phenazine-11-carboxylic acid (dppz-COOH)[34] with biotinylethylenediamine (biotin-en)[35] in DMF at 80 °C. Complexes **1**–**6** were synthesized from the reaction of $[Ir_2(ppy)_4Cl_2]$[15b] with two equivalents of the corresponding diimine ligands in refluxing $MeOH/CH_2Cl_2$ under nitrogen for 4 h, followed by metathesis with KPF_6.[16b,26a] The complexes were purified by column chromatography and recrystallization from a CH_2Cl_2/diethyl ether mixture, and isolated as air-stable orange-to-yellow crystals in good yields. All the complexes were characterized by ^{1}H NMR spectroscopy, positive-ion ESI-MS, IR spectroscopy, and gave satisfactory microanalyses. The amide moieties of complexes **2**, **3**, and **6** were characterized by intense IR absorption bands at approximately 3268–3498 and 1653–1694 cm^{-1}.

X-ray crystal structure determination of complex 4: The perspective drawings of the two independent complex cations of complex **4** are depicted in Figure 1. Selected bond lengths and angles are listed in Table 1. The iridium(III) centers of both cations adopted distorted octahedral geometry. The *trans* angles at the iridium centers ranged from 171.7(9) to 174.5(10)°. In a similar manner to the related iridium(III) complexes,[16c,e,24a,30c,d,f] a *cis* arrangement was observed for the metal–carbon bonds around the iridium(III) centers. The Ir–N bond lengths of the dppz ligands (approximately 2.132(18)–2.19(2) Å) were slightly longer than those of the ppy^- ligands (approximately 2.05(2)–2.14(2) Å), due to the *trans*-influence of the carbon donors. Interestingly, the dppz ligands from two neighboring cations revealed π-stacking interactions with an interplanar separation of about 2.96 Å. The participation of extended planar ligands in π-stacking has also been observed in other dppz and dppn complexes.[6a,9,13]

Electronic absorption and emission properties: The electronic absorption spectral data of complexes **1**–**6** are listed in Table 2. The electronic absorption spectra of complexes **4** and **5** in CH_3CN are shown in Figure 2. All the complexes showed intense intraligand (^{1}IL) (π→π* (diimine and ppy^-)) absorption bands at approximately 243–329 nm (ε of the order of $10^4\ dm^3\,mol^{-1}\,cm^{-1}$). The complexes also displayed less intense absorption shoulders at around 334–497 nm, attributable to spin-allowed metal-to-ligand charge-transfer (^{1}MLCT) (dπ(Ir)→π* (diimine and ppy^-)) transitions.[15a–c,16,18,20d,24a,25,26a,28a,29,30a,c–g] However, for complexes **4**–**6**, the involvement of ^{1}IL (π→π* (diimine)) character in these absorption features cannot be excluded since the free ligands dppz and dppn also absorb in a similar region.[7,8a,9] In addition, all the complexes exhibited weak absorption

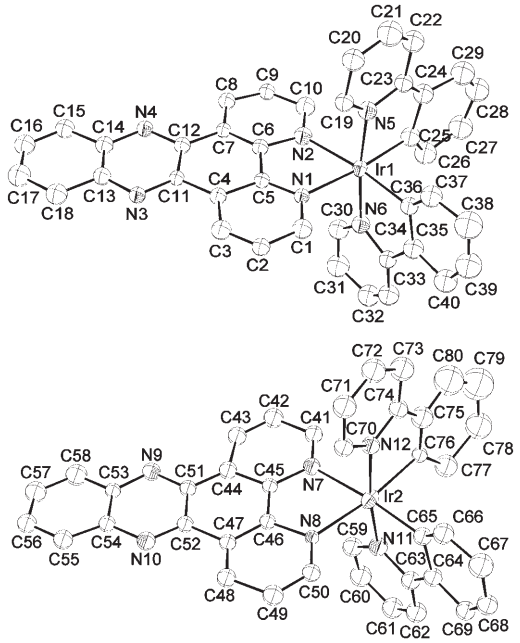

Figure 1. Perspective drawings of the two independent complex cations of complex **4**. The thermal ellipsoids are set at a 20% probability level.

Table 1. Selected bond lengths [Å] and angles [°] for the two independent complex cations of complex **4**.

Ir1–N1	2.132(18)	Ir2–N7	2.19(2)
Ir1–N2	2.18(2)	Ir2–N8	2.169(19)
Ir1–N5	2.10(2)	Ir2–N11	2.05(2)
Ir1–N6	2.09(2)	Ir2–N12	2.14(2)
Ir1–C25	2.06(3)	Ir2–C65	2.05(3)
Ir1–C36	2.08(3)	Ir2–C76	2.10(3)
N1-Ir1-N2	75.7(8)	N7-Ir2-N8	77.4(8)
N1-Ir1-N5	95.8(8)	N7-Ir2-N12	89.0(8)
N1-Ir1-N6	89.0(8)	N7-Ir2-N11	95.9(9)
N1-Ir1-C25	174.4(10)	N7-Ir2-C65	174.5(10)
N1-Ir1-C36	96.8(9)	N7-Ir2-C76	97.1(9)
N2-Ir1-N5	89.1(9)	N8-Ir2-N11	91.0(8)
N2-Ir1-N6	97.1(9)	N8-Ir2-N12	95.7(8)
N2-Ir1-C25	99.8(10)	N8-Ir2-C65	97.5(9)
N2-Ir1-C36	172.3(9)	N8-Ir2-C76	171.7(9)
N5-Ir1-N6	172.9(9)	N11-Ir2-N12	172.4(9)
N5-Ir1-C25	80.8(12)	N11-Ir2-C65	82.2(11)
N5-Ir1-C36	93.5(11)	N11-Ir2-C76	95.8(10)
N6-Ir1-C25	94.8(12)	N12-Ir2-C65	93.4(10)
N6-Ir1-C36	80.8(11)	N12-Ir2-C76	77.9(10)
C25-Ir1-C36	87.8(11)	C65-Ir2-C76	88.2(10)

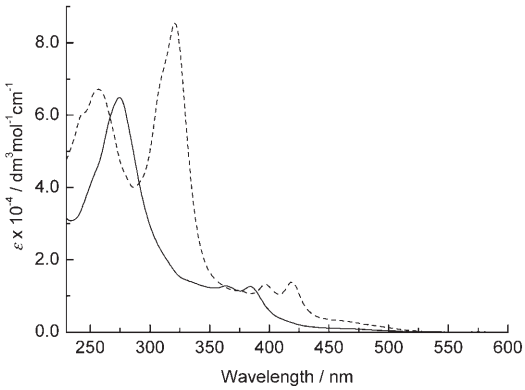

Figure 2. Electronic absorption spectra of complexes **4** (——) and **5** (-----) in CH_3CN at 298 K.

tails towards the lower energy region (at about 502–550 nm), that are tentatively assigned to spin-forbidden ^{3}MLCT (dπ(Ir)→π* (diimine and ppy$^-$)) transitions.[15a–c,16,18,20d,24a,25,26a,28a,29,30a,c–g]

Upon photoexcitation, complexes **1**–**6** displayed long-lived green-to-orange luminescence under ambient conditions and in alcohol glass at 77 K. The emission data are summarized in Table 3. The emission spectra of the dppz complex **4** and the dppzB complex **6** in fluid solutions at 298 K and in EtOH/MeOH glass at 77 K are shown in Figures 3 and 4, respectively. The emission of complexes **1**–**5** in fluid solutions is assigned to an ^{3}MLCT (dπ(Ir)→π* (diimine)) excited state.[15,16b,e,18a,19b,20a,b,d,24a,25a,b,26a,28a,29b,30a,c–f] The assignment of a charge-transfer excited state is supported by the shorter emission lifetimes and lower emission quantum yields of the complexes in more polar solvents such as CH_3CN and MeOH than in the less polar CH_2Cl_2 solvent (Table 3). These observations are common to other iridium(III) MLCT emitters.[15,16b,18a,19b,20a,b,d,24a,30a,c–f] Among complexes **1**–**3**, it is interesting to note that the decrease of the emission quantum yield on going from CH_2Cl_2 to MeOH was much more significant for the amido complexes **2** and **3** compared with the dpq complex **1** (Table 3). In aqueous buffer, complex **1** emitted very weakly whereas complexes **2** and **3** were non-emissive. It is likely that the reduced quantum yields of complexes **2** and **3** are due to the possible hydrogen-bonding

Table 2. Electronic absorption spectral data for complexes **1**–**6** at 298 K.

Complex	Medium	λ_{abs} [nm] (ε_{max} [dm^{3}mol^{-1}cm^{-1}])
1	CH_2Cl_2	258 (78070), 295 sh (34005), 337 sh (11015), 358 sh (8365), 382 (8165), 420 (2980), 467 sh (925)
	MeOH	257 (74365), 293 sh (31555), 335 sh (10650), 355 sh (8230), 375 (7320), 414 sh (3170), 467 sh (850)
2	CH_2Cl_2	254 sh (64000), 262 (75865), 296 sh (34535), 363 sh (8840), 385 sh (7790), 467 sh (895)
	MeOH	252 sh (56385), 261 (67595), 297 sh (31130), 360 sh (8635), 383 sh (6915), 465 sh (830)
3	CH_2Cl_2	255 sh (74265), 262 (83835), 298 sh (37435), 361 sh (10095), 383 sh (8810), 411 sh (4365), 468 sh (1035)
	MeOH	253 sh (64675), 261 (73725), 299 sh (33650), 361 sh (9635), 381 sh (8025), 468 sh (950)
4	CH_2Cl_2	254 sh (80320), 269 sh (74900), 280 (82990), 366 (16985), 389 (16320), 467 sh (1195), 497 sh (850)
	CH_3CN	275 (64890), 334 sh (13810), 364 (12680), 385 (12660), 468 sh (850)
5	CH_2Cl_2	245 sh (59935), 260 (72100), 313 sh (58465), 329 (82515), 379 sh (14350), 401 (14850), 424 (14720), 470 sh (3645)
	CH_3CN	243 sh (60315), 257 (67190), 307 sh (66155), 321 (85445), 375 sh (11905), 397 (13565), 419 (14205), 465 sh (3230)
6	CH_2Cl_2	252 sh (53755), 269 sh (71085), 282 (82540), 338 sh (18940), 372 (18450), 393 (16560), 466 sh (1255), 502 sh (810)
	CH_3CN	250 sh (54195), 268 sh (77855), 277 (87360), 336 sh (18810), 369 (18220), 388 (17140), 467 sh (1230)

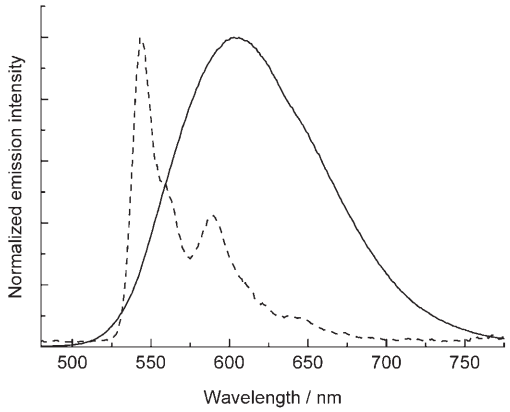

Figure 3. Emission spectra of complex **4** in CH_2Cl_2 at 298 K (——) and EtOH/MeOH 4:1 at 77 K (-----).

interactions between the amide groups of the diimine ligands and protic solvent molecules.[3a] Among the dppz and dppn complexes **4**–**6**, we found that complexes **4** and **6** also showed solvent-dependent emission quantum yields (Table 3). Both of these complexes did not emit in aqueous solution. Hydrogen-bonding interactions between the phenazine nitrogen atoms of both complexes (and the amide moiety of complex **6**) and water molecules may also exist.[4a–e,g] However, the dppn complex **5** did not display similar solvent-dependent emission but exhibited very similar emission lifetimes and quantum yields in different solvents. It is probable that the excited state of this complex has substantial ^{3}IL ($\pi\rightarrow\pi^*$ (dppn)) character. Unlike complexes **1**–**5**, dppzB complex **6** displayed dual emission in fluid solutions at room temperature. Every effort was made to check the purity of the sample to ensure that the emission was not due to the presence of impurities. The purity of the samples has been confirmed by the characterization data, elemental analysis, and HPLC analysis. Specifically, the emission spectrum of complex **6** in CH_2Cl_2 displayed two bands at 510 and 654 (sh) nm (Figure 4). Excitation spectra monitored at these two emission wavelengths were similar, with broad bands at around 340 and 410 nm; this indicates that both emission bands are from the same species. The higher-energy emission band at approximately 510 nm is tentatively assigned to an excited state of ^{3}IL ($\pi\rightarrow\pi^*$ (dppzB)) character in view of its longer emission lifetime ($\tau_o = 0.71$ μs) and structural features. The lower-energy emission shoulder was of a shorter lifetime ($\tau_o = 0.13$ μs) and appeared at about 654 nm, and is lower in energy compared with the emission band of the dppz complex **4** (around 603 nm) under similar conditions. It is likely that this emission is derived from an excited state of ^{3}MLCT ($d\pi(Ir)\rightarrow\pi^*$ (dppzB)) character. The occurrence of this band at lower energy than that of the dppz complex **4** is due to the presence of the electron-withdrawing amide group in the dppzB ligand. Similar dual luminescence was observed in other solvents such as MeOH and CH_3CN (Figure 4). The ^{3}IL emission occurred at 490–556 nm ($\tau_o = 1.71$–1.40 μs) and the ^{3}MLCT emission at 612–650 nm (sh) ($\tau_o = 0.83$–0.36 μs).

Table 3. Photophysical data for complexes **1**–**6**.

Complex	Medium (T[K])	λ_{em}[nm]	τ_o[μs]	Φ_{em}
1	CH_2Cl_2 (298)	590	0.67	0.24
	CH_3CN (298)	601	0.34	0.11
	MeOH (298)	603	0.18	0.064
	glass[a] (77)	528, 561 sh	4.72	
2	CH_2Cl_2 (298)	599	0.48	0.17
	CH_3CN (298)	608	0.13	0.034
	MeOH (298)	598	1.46 (8%), 0.14 (92%)	0.0009
	glass[a] (77)	532, 566 sh	3.86	
3	CH_2Cl_2 (298)	597	0.43	0.13
	CH_3CN (298)	606	0.09	0.019
	MeOH (298)	596	1.13 (7%), 0.15 (93%)	0.0006
	glass[a] (77)	529, 565 sh	3.93	
4	CH_2Cl_2 (298)	603	0.56	0.072
	CH_3CN (298)	630	0.077	0.0023
	MeOH (298)	600	0.38	$<10^{-4}$
	glass[a] (77)	544 (max), 563 sh, 589, 643 sh	1224	
5	CH_2Cl_2 (298)	585	0.58	0.0016
	CH_3CN (298)	588	0.36	0.0012
	MeOH (298)	583	0.42	0.0016
	glass[a] (77)	535	4.45	
6	CH_2Cl_2 (298)	510, 535 sh	0.71	0.019
		654 sh	0.13	
	CH_3CN (298)	492 sh, 520	1.40	0.0064
		612 sh	0.83	
	MeOH (298)	490, 530, 556 (max)	1.71	0.0010
		650 sh	0.36	
	glass[a] (77)	547 (max), 591, 644 sh	1040	

[a] EtOH/MeOH 4:1.

Upon cooling to low temperature, most of the complexes displayed a significant blue shift in the emission maxima (Table 3). The blue shifts indicate that ^{3}MLCT ($d\pi(Ir)\rightarrow\pi^*$ (diimine)) character exists in the excited states of these complexes at low temperature. The emission spectra of the dppz complex **4** and dppzB complex **6** in alcohol glass showed rich vibronic features with progressional spacings of about 1362–1426 cm^{-1} (Figures 3 and 4), and their emission lifetimes approached 1 ms. These observations suggest that the emissive state of these complexes at low temperature possessed predominant ^{3}IL ($\pi\rightarrow\pi^*$ (dppz or dppzB)) character. Similar vibronically structured emission has also been

observed for related rhenium(I)–dppz complexes in alcohol glass at 77 K.[7,8a,9,10]

Electrochemical properties: The electrochemical properties of complexes **1–6** have been studied by cyclic voltammetry. The electrochemical data are collected in Table 4. The cyclic voltammograms of all the complexes showed a reversible/quasi-reversible oxidation couple at about +1.26 V versus SCE, that is assigned to metal-centered Ir^{IV}/Ir^{III} oxidation.[15a,b,16b,d,e,20a,24b,25b,28a,30a,c–g] The complexes exhibited the first and second reduction couples at around −0.76 to −1.26 V and −1.20 to −1.72 V versus SCE, respectively (Table 4). With reference to previous studies,[15a,b,,16a,b,d,e,18,20a,24a,b,25b,26a,30a,c–g] these couples are assigned to the reduction of the diimine ligands. This assignment is substantiated by the fact that the first two reduction couples of the amido dpq complexes **2** and **3** (≈−1.1 and −1.5 V) occurred at less negative potentials than those of the dpq complex **1** (−1.26 and −1.72 V). These observations are attributed to the electron-withdrawing properties of the amide group of the ligands dpqa and dpqB. In addition, the first two reduction couples of the dppn complex **5** (−0.76 and −1.20 V) occurred at less negative potentials than those of the dppz complex **4** (−0.98 and −1.50 V) owing to the more conjugated dppn ligand of the former complex. The first two reduction couples of the dppzB complex **6** (−0.85 and −1.34 V) also occurred at less negative potentials than those of the dppz complex **4** because of the presence of the electron-withdrawing amide group in the dppzB ligand. All the complexes underwent reductions at more negative potentials that are assigned to the reduction of the diimine and cyclometalating ligands.[15a,b,16a,b,d,e,18,20a,24a,b,25b,26a,30a,c–g]

Table 4. Electrochemical data for complexes **1–6**.[a]

Complex	Oxidation $E_{1/2}$ or E_a [V]	Reduction $E_{1/2}$ or E_c [V]
1	+1.26	−1.26, −1.72,[b] −2.05,[c] −2.46,[c] −2.67[c]
2	+1.27	−1.10, −1.54, −2.08,[c] −2.26,[c] −2.70
3	+1.26	−1.08, −1.55,[c] −2.26[c]
4	+1.26	−0.98, −1.50, −1.68, −2.13[c]
5	+1.27[b]	−0.76, −1.20,[b] −1.65, −2.10[c]
6	+1.27[b]	−0.85, −1.34, −1.75,[c] −2.39[c]

[a] In CH_3CN (0.1 mol dm^{-3} TBAP) at 298 K, glassy carbon electrode, sweep rate 0.1 V s^{-1}, all potentials versus SCE. [b] Quasi-reversible couple. [c] Irreversible wave.

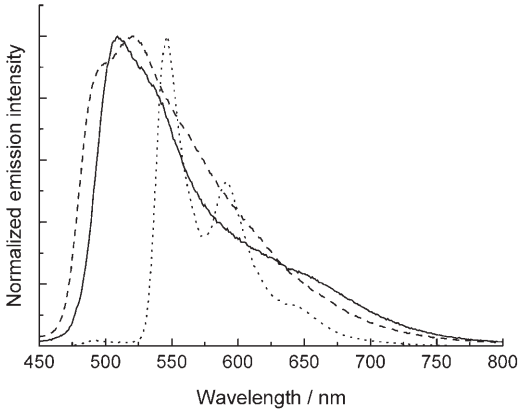

Figure 4. Emission spectra of complex **6** in CH_2Cl_2 (——) and CH_3CN (-----) at 298 K, and EtOH/MeOH 4:1 at 77 K (•••••).

DNA-binding studies

Electronic absorption titrations: The interactions of complexes **1–6** with double-stranded calf thymus DNA have been investigated by electronic absorption titrations. Complexes **1–3** and **6** did not show any changes in their absorption spectra in the presence of double-stranded DNA. However, the absorption bands of the dppz complex **4** at approximately 366 and 386 nm, and the dppn complex **5** at around 322, 397, and 419 nm exhibited hypochromism and bathochromic shifts upon addition of double-stranded calf thymus DNA. The electronic absorption spectra of the dppn complex **5** in the absence and presence of double-stranded calf thymus DNA are shown in Figure 5. These results indicate

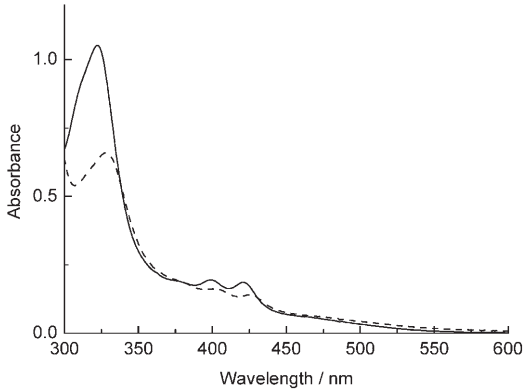

Figure 5. Electronic absorption spectra of complex **5** (12 μM) in a mixture of Tris-Cl buffer (50 mM, pH 7.4) and methanol (7:3) in the absence (——) and presence (-----) of double-stranded calf thymus DNA (671 μM).

that these complexes bind to the double-stranded DNA molecules, probably through a non-covalent intercalative binding mode.[36] Similar spectral changes have been observed in other transition-metal dppz and dppn complexes.[4a–e,5,6c,7–13]

The data obtained from the absorption titration experiments have been fitted by using Equations (1) and (2) developed by Bard[37] and Thorp[6b,c] to estimate the intrinsic bind-

ing constants (K) and binding site sizes (s) for complexes **4** and **5**:

$$\frac{(\varepsilon_a-\varepsilon_f)}{(\varepsilon_b-\varepsilon_f)} = \frac{\left(b-\sqrt{b^2-\frac{2K^2c_t[\mathrm{DNA}]}{s}}\right)}{2Kc_t} \quad (1)$$

$$b = 1 + Kc_t + \frac{K[\mathrm{DNA}]}{2s} \quad (2)$$

where ε_a is the extinction coefficient observed for the absorption band at a DNA concentration [DNA]; ε_b is the extinction coefficient of the fully bound species; ε_f is the extinction coefficient of free complex and c_t is the total concentration of the metal complex. The plot of $(\varepsilon_a-\varepsilon_f)/(\varepsilon_b-\varepsilon_f)$ against [DNA] for the dppn complex **5** is shown in Figure 6.

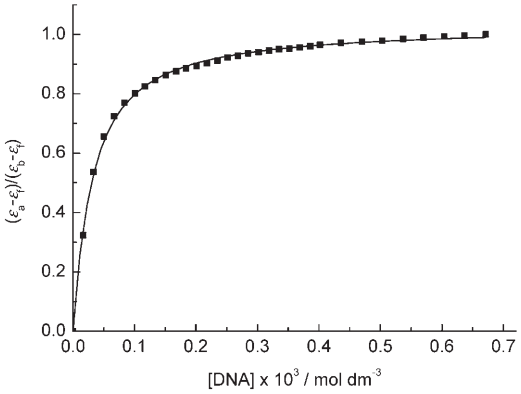

Figure 6. Plot of $(\varepsilon_a-\varepsilon_f)/(\varepsilon_b-\varepsilon_f)$ against [DNA] for the binding of complex **5** (12 μM) to double-stranded calf thymus DNA. The experimental data at $\lambda_{abs}=322$ nm were fitted by using Equations (1) and (2).

The intrinsic binding constants were determined to be 2.0×10^4 ($s=1.3$) and $7.8\times10^4\,\mathrm{M}^{-1}$ ($s=1.4$) for the binding of the dppz complex **4** and dppn complex **5** to double-stranded calf thymus DNA, respectively (Table 5). The binding constants of the complexes are smaller than those observed for $[(\eta^5\text{-}C_5Me_5)Ir(N\text{-acetyl-L-cysteine})(dppz)]^+$ ($K=8.8\times10^4\,\mathrm{M}^{-1}$)[13a] and [*fac*-Re(dppz)(CO)$_3$(4-MePy)]$^+$ (4-MePy = 4-methylpyridine) ($K=6.0\times10^6\,\mathrm{M}^{-1}$),[7] which could be due to the higher MeOH content of the titration buffer in the current work.[38] The constants are also smaller than the binding constant of $[Ru(bpy)_2(dppz)]^{2+}$ ($K=4.0\times10^6\,\mathrm{M}^{-1}$).[6b] Thus, the diminished binding strength can also be due to the lower cationic charge of the current iridium(III) complexes. The binding constant of the dppn complex **5** is larger than that of the dppz complex **4**. It is likely that the enhanced binding affinity is due to the larger planar surface area of the dppn ligand. Similar observations have been reported for related rhenium(I)–dppz and –dppn complexes.[9,10]

Emission titrations: The DNA-binding properties of all the iridium(III) complexes have been studied by emission titrations. Of the six complexes, the biotin-free complexes **1**, **2**, **4**, and **5** displayed emission enhancement in the presence of double-stranded calf thymus DNA. The emission intensity of the dpq complex **1** at about 591 nm was enhanced by approximately 33-fold (Figure 7). Both the dpqa complex **2** and the dppz complex **4** did not emit in aqueous buffer solution. However, upon addition of double-stranded DNA, new emission bands were observed at around 602 and 606 nm for these two complexes, respectively (Figures 8 and 9). The emission intensities of the new emission bands were approx-

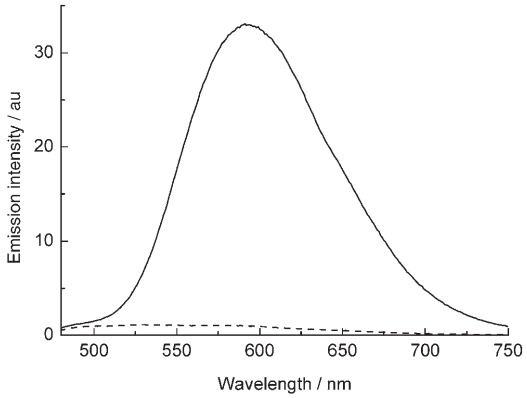

Figure 7. Emission spectra of complex **1** (137 μM) in a mixture of Tris-Cl buffer (50 mM, pH 7.4) and methanol (7:3) in the absence (-----) and presence (——) of double-stranded calf thymus DNA (744 μM).

Table 5. DNA-binding parameters for complexes **1–6** in a mixture of Tris-Cl buffer (50 mM, pH 7.4) and methanol (7:3) at 298 K.[a]

Complex	Intrinsic binding constant, K [M^{-1}] (binding site size, s)					
	absorption titrations			emission titrations		
	calf thymus DNA	poly(dA)·poly(dT)	poly(dG)·poly(dC)	calf thymus DNA	poly(dA)·poly(dT)	poly(dG)·poly(dC)
1	[b]	[b]	[b]	1.2×10^4 (1.6)	1.9×10^4 (0.7)	3.0×10^4 (0.6)
2	[b]	[b]	[b]	1.1×10^4 (1.5)	1.1×10^4 (0.7)	[c]
3	[b]	[b]	[b]	[b]	[b]	[b]
4	2.0×10^4 (1.3)	2.3×10^4 (1.7)	1.0×10^4 (1.1)	2.4×10^4 (1.6)	3.0×10^4 (1.9)	1.5×10^4 (1.3)
5	7.8×10^4 (1.4)	7.6×10^4 (1.2)	5.0×10^4 (1.0)	[c]	[c]	[c]
6	[b]	[b]	[b]	[b]	[b]	[b]

[a] The trifluoromethanesulfonate salts of complexes **4** and **5** were used for the absorption and emission titration experiments due to their higher solubilities. [b] No observable changes. [c] The binding parameters could not be accurately determined due to the low increase in emission intensity and unsatisfactory fits.

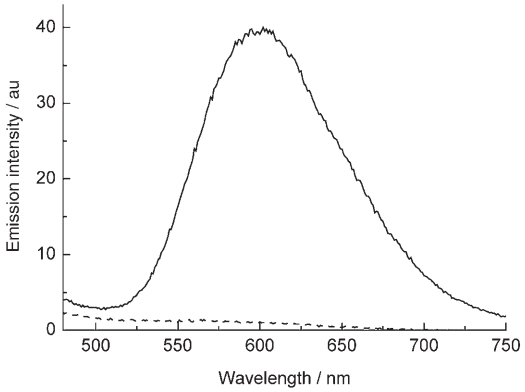

Figure 8. Emission spectra of complex **2** (124 μM) in a mixture of Tris-Cl buffer (50 mM, pH 7.4) and methanol (7:3) in the absence (-----) and presence (——) of double-stranded calf thymus DNA (114 μM).

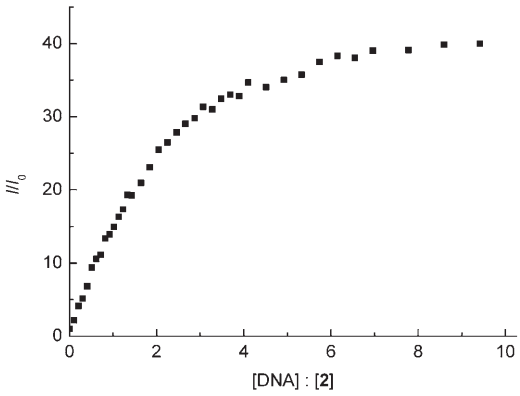

Figure 10. Emission titration curve for the titrations of complex **2** (124 μM) with double-stranded calf thymus DNA. The emission intensity of complex **2** was monitored at 602 nm.

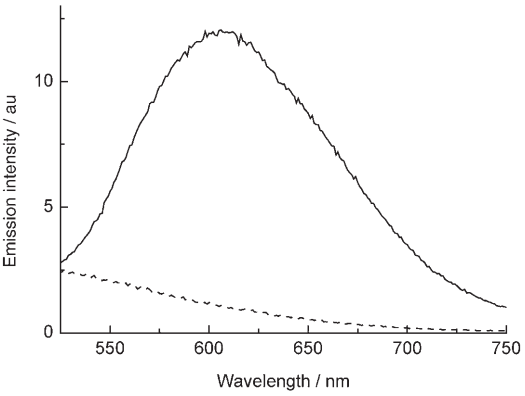

Figure 9. Emission spectra of complex **4** (85 μM) in a mixture of Tris-Cl buffer (50 mM, pH 7.4) and methanol (7:3) in the absence (-----) and presence (——) of double-stranded calf thymus DNA (238 μM).

imately 40- and 12-times that of the background in the absence of DNA. The emission enhancement is ascribed to the intercalation of the complexes to the base-pairs of the double-stranded DNA molecules. In general, intercalation results in: i) the protection of the diimine ligands from interacting with the water molecules; ii) a more hydrophobic environment; iii) a higher rigidity of the local surroundings of the complexes. All these factors would lead to enhanced emission intensity. The emission titration curve for the dpqa complex **2** with calf thymus DNA is displayed in Figure 10. The data from the emission titrations were fitted by using Equations (1) and (2) to determine the binding parameters. Fitting of the titration data for the dpq complex **1**, dpqa complex **2**, and dppz complex **4** gave intrinsic binding constants of 1.2×10^4 ($s=1.6$), 1.1×10^4 ($s=1.5$) and 2.4×10^4 M^{-1} ($s=1.6$), respectively (Table 5). The binding constants for the dpq complex **1** and dpqa complex **2** are smaller than those observed for $[Ru(bpy)_2(dpq)]^{2+}$ ($K=5.9\times10^4\,M^{-1}$) and $[Ru(bpy)_2(dpqC)]^{2+}$ (dpqC = dipyrido[3,2-*a*:2′,3′-*c*](6,7,8,9-tetrahydro)phenazine) ($K=8.5\times10^4\,M^{-1}$).[4g] Again, the diminished binding affinity is attributed to the higher MeOH content of the titration buffer and the lower cationic charge of the complexes. The binding constant for the dppz complex **4** is similar to that obtained by absorption titrations (Table 5), which is approximately two orders of magnitude smaller than the K values of other dppz complexes such as $[Ru(bpy)_2(dppz)]^{2+}$ ($K=4.0\times10^6\,M^{-1}$).[6b] The DNA-induced emission enhancement of the dppn complex **5** was relatively small (< four-fold approximately) and no satisfactory fits could be obtained from the emission data. Similarly small emission enhancement has also been observed for $[Ru(phen)_2(dppn)]^{2+}$ and it was ascribed to the insensitivity of the luminescence of this complex to its local environment.[4a] The small increase of emission intensity of complex **5** is also in line with our findings that the luminescence quantum yields of this complex were not very sensitive to the solvent polarity (Table 3). Nevertheless, the intercalative binding of complex **5** to double-stranded DNA is justified by the observed changes in absorption titrations (Figure 5).

Although the photophysical properties of the biotin complexes **3** and **6** were very similar to those of their dpq and dppz counterparts (complexes **1** and **4**), respectively, their spectra did not show any changes in the DNA titration experiments. These observations are probably a result of the steric bulk of the biotin moiety that prevents the complexes from intercalating into the double-stranded DNA molecules.

Synthetic DNA-binding studies

Electronic absorption titrations: To examine the possible DNA-sequence selectivity of the intercalating complexes, absorption titration experiments using the synthetic double-stranded oligonucleotides poly(dA)·poly(dT) and poly(dG)·poly(dC) have been performed. Similar to the case of calf thymus DNA, the low-energy absorption bands of the dppz complex **4** and dppn complex **5** exhibited hypochromism and bathochromic shifts upon addition of the synthetic double-stranded oligonucleotides. The binding affinities of the dppz complex **4** to poly(dA)·poly(dT) and poly(dG)·poly(dC) were determined to be $2.3\times10^4\,M^{-1}$ ($s=1.7$) and $1.0\times10^4\,M^{-1}$ ($s=1.1$), respectively (Table 5). The binding parame-

ters of the dppn complex **5** to poly(dA)·poly(dT) ($K=7.6\times10^4\,\text{M}^{-1}$, $s=1.2$) and poly(dG)·poly(dC) ($K=5.0\times10^4\,\text{M}^{-1}$, $s=1.0$) have also been determined (Table 5). The binding affinities of these two complexes to calf thymus DNA (GC content = 42 %)[39] are comparable to those to poly(dA)·poly(dT) but higher than those to poly(dG)·poly(dC) (Table 5). Similar selective binding has been observed for related osmium(II) complexes.[4e]

Emission titrations: The emission intensity of the dpq complex **1** was enhanced by approximately 38- and 30-fold upon addition of poly(dA)·poly(dT) and poly(dG)·poly(dC), respectively. Fitting of the titration data gave intrinsic binding constants of 1.9×10^4 ($s=0.7$) and $3.0\times10^4\,\text{M}^{-1}$ ($s=0.6$) for poly(dA)·poly(dT) and poly(dG)·poly(dC), respectively (Table 5). Interestingly, these values reveal that complex **1** binds to poly(dG)·poly(dC) with a slightly higher affinity. Such binding preference has been reported for a ruthenium(II)–dppz complex $[\text{Ru(tpm)(py)(dppz)}]^{2+}$ (tpm = tris-(1-pyrazolyl)methane; py = pyridine), the binding constant of which for poly(dG)·poly(dC) is an order of magnitude larger than that for poly(dA)·poly(dT).[8b] For the dpqa complex **2**, the emission intensity was increased by approximately 46-fold in the presence of poly(dA)·poly(dT). The binding constant and site size determined from Equations (1) and (2) were $1.1\times10^4\,\text{M}^{-1}$ and 0.7, respectively, and are similar to those for calf thymus DNA (Table 5). Unfortunately, only small emission enhancement (< five-fold approximately) was observed when poly(dG)·poly(dC) was used and no satisfactory fits were obtained. The binding parameters could not be determined from the emission titration data with accuracy.

The emission intensity of the dppz complex **4** was enhanced by about 17-fold upon addition of poly(dA)·poly(dT). The emission enhancement induced by poly(dG)·poly(dC) was slightly smaller (approximately 14-fold). The binding affinities for complex **4** to poly(dA)·poly(dT) ($K=3.0\times10^4\,\text{M}^{-1}$ and $s=1.9$) and poly(dG)·poly(dC) ($K=1.5\times10^4\,\text{M}^{-1}$ and $s=1.3$) are also in agreement to those determined from absorption titrations (Table 5). The higher binding affinity to poly(dA)·poly(dT) than poly(dG)·poly(dC) is also similar to the results obtained in absorption titrations. The dppn complex **5**, again, showed only small emission enhancement (< two-fold approximately) upon addition of synthetic DNA, which is ascribed to the insensitivity of the emission of this complex to its surroundings.

Avidin-binding studies

The avidin-biotin system has been widely used in various bioanalytical applications owing to the extremely strong binding affinity of biotin to avidin (first dissociation constant, $K_d=\approx10^{-15}\,\text{M}$).[40,41] Recently, we have reported the use of transition-metal biotin complexes as luminescent probes for avidin.[10,30e,g,42] Emission increase and lifetime elongation are both observed when the complexes bind to the hydrophobic binding sites of avidin. We anticipated that by attaching a biotin moiety to iridium(III)–dpq and –dppz complexes, specific and sensitive luminescent probes for avidin could be obtained. In view of this, the dpqB complex **3** and dppzB complex **6**, both containing a biotin moiety, have been designed. The avidin-binding properties of the complexes have been studied by using HABA assays and emission titrations.

HABA assays: The assays are based on the competition between biotin and HABA on binding to the substrate-binding sites of avidin. The binding of HABA to avidin is associated with an absorption feature at approximately 500 nm. Since the binding of HABA to avidin (first dissociation constant, $K_d=6\times10^{-6}\,\text{M}$) is much weaker than that of biotin ($K_d=\approx10^{-15}\,\text{M}$), addition of biotin replaces the bound HABA molecules, leading to a decrease of the absorbance at 500 nm. Addition of complex **3** or **6** to a mixture of HABA and avidin decreased the absorbance at 500 nm; this indicates the displacement of HABA from the avidin molecules. Nonspecific displacement of HABA from the biotin-binding site was excluded since no absorption change was observed when complex **1**, **2**, **4**, or **5** was added. The plots of $-\Delta A_{500\,\text{nm}}$ against [Ir]:[avidin] for complexes **3** and **6** showed that the equivalence points occurred at [Ir]:[avidin] ≈4.3 and 5.4, respectively. These values are larger than those of other iridium–biotin complexes in our previous studies.[30e,g] These results show that the binding of complexes **3** and **6** to avidin is not substantially stronger than that of HABA.

Avidin emission titrations: Both the dpqB complex **3** and dppzB complex **6** were non-emissive in aqueous buffer. However, addition of avidin to complex **3** or **6** in a mixture of potassium phosphate buffer (50 mM, pH 7.4) and MeOH (9:1) led to the appearance of a new emission band with a maximum at 490 nm and a shoulder at around 520 nm. The emission spectra of complex **3** in the absence and presence of avidin are displayed in Figure 11. At a ratio of [Ir]:[avidin] = 4, the emission intensities of complexes **3** and **6** at 490 nm were increased by approximately 31- and 8-fold, re-

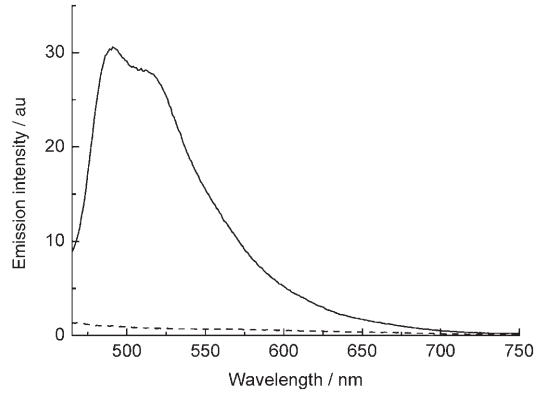

Figure 11. Emission spectra of complex **3** (22 μM) in a mixture of potassium phosphate buffer (50 mM, pH 7.4) and methanol (9:1) in the absence (-----) and presence (——) of avidin (5.5 μM).

spectively. The emission enhancement is attributed to the specific binding of the biotin moiety of complexes **3** and **6** to avidin since such emission enhancement was not observed for the biotin-free complexes **1**, **2**, **4**, and **5** or when avidin pre-blocked with biotin was added to complexes **3** and **6**. Interestingly, the emission band of the adduct $\mathbf{3}_4$-avidin occurred at much higher energy compared with the free complex in organic solvents (about 596–606 nm) (Table 3) and the DNA-adducts of the dpq complex **1** and dpqa complex **2** (around 591 and 602 nm, respectively) (Figures 7 and 8). Although avidin-induced emission enhancement of luminescent transition-metal biotin complexes has been observed, the emission energy did not change significantly.[10,30e,g,42] The appearance of a new emission band for this iridium(III)–biotin complex at higher energy could be partly due to the hydrophobic biotin-binding site of the protein because many cyclometalated iridium(III)–diimine complexes possess solvatochromic behavior.[15,16a–c,e,18,19b,20,24a,b,30a,c–f] However, complex **3** did not show very different emission wavelengths in different solvents (Table 3), and such a large difference in emission energy (approximately 3755 cm^{-1}) compared to the DNA adduct of the dpqa complex **2**, which has the same luminophore, cannot be solely due to hydrophobic effects. The occurrence of this high-energy emission band cannot be fully ascribed to rigidochromic effects either. The reason is that the emission maximum of the complex **3** in rigid glass occurred at 529 nm (Table 3), that is still of significantly lower energy compared to that of the emission maximum of $\mathbf{3}_4$-avidin in buffer solution (490 nm). Thus, the most probable reason for the blue-shift is that the emission of this adduct originates from a state of higher energy than the MLCT state, that is likely to be a state of predominant ^{3}IL ($\pi\rightarrow\pi^*$(dpqB)) character. This assignment is supported by the long emission lifetime (about 2.20 μs) and the vibronic features of the emission band, that showed a spacing of 1177 cm^{-1}. In addition, the uncoordinated dpqB ligand displayed vibronic emission at $\lambda_{max}\approx480$ nm in alcohol glass (progressional spacings of approximately 1378 cm^{-1}). The reason for the switching of excited-state nature from supposedly ^{3}MLCT ($d\pi$(Ir)$\rightarrow\pi^*$(dppzB)) to ^{3}IL ($\pi\rightarrow\pi^*$(dppzB)) is unknown at this stage. However, these findings could be unique to cyclometalated iridium(III)–polypyridine complexes because the ^{3}IL/^{3}MLCT emission of these complexes responds very sensitively to subtle changes of the identity of the cyclometalating and polypyridine ligands as well as their local environments.

Emission titration studies showed that the adduct $\mathbf{6}_4$-avidin showed a structured emission band at around 490 nm (a spacing of 1177 cm^{-1}) with a lifetime of 1.78 μs. We tentatively assign this band to an excited state of ^{3}IL ($\pi\rightarrow\pi^*$(dppzB)) character. The assignment is supported by the observation of the ^{3}IL emission of complex **6** at similar energy in organic solvents (Table 3).

Determination of k_{on}, k_{off}, and K_d: The first dissociation constants K_d of complexes **3** and **6** were determined from the on- and off-rate constants of the iridium–avidin adducts from kinetics experiments.[43] The K_d of complexes **3** and **6** were determined to be 2.0×10^{-7} and 8.2×10^{-7} M, respectively (Table 6). The K_d values of the complexes are approximately 8–9 orders of magnitude larger than that of native biotin ($K_d = \approx10^{-15}$ M)[40,41] and 1–3 orders of magnitude larger than those of other iridium–biotin complexes in our previous studies.[30e,g] This indicates that the binding of the current iridium(III)–biotin complexes to avidin is hindered by the extended planar moieties of the dpqB and dppzB ligands. The larger dissociation constants of these iridium(III)–biotin complexes are also a consequence of the relatively short spacer-arms between the iridium(III) complex and the biotin moiety.

Table 6. On- and off-rate constants for complexes **3** and **6** and first dissociation constants for the iridium(III)–avidin adducts in potassium phosphate buffer (50 mM, pH 7.4) at 298 K.

Complex	k_{on} [$M^{-1}min^{-1}$]	k_{off} [min^{-1}]	K_d [M]
3	1.1×10^4	2.2×10^{-3}	2.0×10^{-7}
6	6.7×10^3	5.5×10^{-3}	8.2×10^{-7}

Conclusion

A new class of luminescent iridium complexes containing different extended planar ligands has been synthesized. The DNA-binding properties of the complexes have been investigated by absporption and emission titrations. The results suggested that the dpq, dpqa, dppz, and dppn complexes bind to the double-stranded DNA through an intercalative binding mode. The avidin-binding properties of the biotin-containing complexes have also been investigated by HABA and emission titrations. Remarkably, unlike the DNA-adducts of related complexes, upon binding to avidin, these biotin complexes emitted from an intraligand triplet excited state. These interesting findings could be useful in the design of biomolecule-specific luminescent probes.

Experimental Section

General comments and instrumentation: All solvents were of analytical reagent grade and purified according to standard procedures.[44] All buffer components were of biological grade and used as received. $IrCl_3{\cdot}3H_2O$ (Aldrich), Hppy (Aldrich), 2,3-diaminonaphthalene (Acros), CDI (Acros), biotin (Acros), and KPF_6 (Acros) were used without purification. 1,2-Diaminobenzene (Acros) was purified by sublimation. Ethylenediamine (Sigma) and *n*-butylamine (Aldrich) were purified by distillation. 2-(Methoxycarbonyl)dipyrido[3,2-*f*:2′,3′-*h*]quinoxaline,[31] biotin-NHS,[33] dppz-COOH,[34] biotin-en,[35] dpq,[2b] dpqa,[31] dppz,[32] and dppn[32] were synthesized according to literature procedures. Tetra-*n*-butylammonium hexafluorophosphate (TBAP) was obtained from Aldrich and was recrystallized from hot EtOH and dried in vacuo at 110 °C before being used. Double-stranded calf thymus DNA was obtained from Calbiochem and purified by phenol extraction as described.[45] Synthetic double-stranded oligonucleotides poly(dA)·poly(dT) and poly(dG)·poly(dC) (Amersham Biosciences) were used as received. The DNA concentration per base-pair was determined from absorption spectroscopy

using the following extinction coefficients ($dm^3 mol^{-1} cm^{-1}$) at the indicated wavelengths: calf thymus DNA, $\varepsilon_{260\,nm}=6600$; poly(dA)·poly(dT), $\varepsilon_{260\,nm}=6000$; and poly(dG)·poly(dC), $\varepsilon_{253\,nm}=7400$.[46] The instrumentation for physical measurements has been described previously.[30d] Luminescent quantum yields were measured using the optically dilute method[47] with an aerated aqueous solution of $[Ru(bpy)_3]Cl_2$ ($\Phi_{em}=0.028$)[48] as the standard solution.

Synthesis of dpq-en: A mixture of 2-(methoxycarbonyl)dipyrido[3,2-*f*:2′,3′-*h*]quinoxaline (500 mg, 1.72 mmol) and ethylenediamine (5.8 mL, 86 mmol) in MeOH (250 mL) was stirred under an inert atmosphere of nitrogen for five days. The yellow solution was then evaporated to dryness under vacuum. The solid was washed with CH_2Cl_2 and diethyl ether. Subsequent recrystallization of the product from a MeOH/diethyl ether mixture afforded a yellow solid (548 mg, 99%). Positive-ion ESI-MS ion clusters at *m*/*z* [M^+]: 319 [dpq-en+H]$^+$.

DpqB: A mixture of dpq-en (200 mg, 0.63 mmol) and biotin-NHS (236 mL, 0.69 mmol) in DMF (45 mL) was heated at 60 °C under an inert atmosphere of nitrogen for 12 h. The pale yellow solution was then evaporated to dryness under vacuum. The solid was washed with isopropanol and diethyl ether. Subsequent recrystallization of the product from a MeOH/diethyl ether mixture afforded pale brown crystals (140 mg, 41%). ^{1}H NMR (300 MHz, CD_3OD, 298 K, TMS): $\delta=9.94$–9.86 (m, 1H; H_c), 9.65 (s, 1H; H_d), 9.56 (d, $J=7.6$ Hz, 1H; H_e), 9.26–9.20 (m, 2H; H_a, H_g), 8.20–7.92 (m, 2H; H_b, H_f), 4.51–4.47 (m, 1H; NCH biotin), 4.32–4.28 (m, 1H; NCH biotin), 3.68–3.60 (m, 4H; NH(CH_2)$_2$NH), 3.28–3.17 (m, 1H; SCH biotin), 2.93 (dd, $J=12.6$, 5.0 Hz, 1H; SCH biotin), 2.70 (d, $J=14.1$ Hz, 1H; SCH biotin), 2.33–2.15 (m, 2H; COCH_2 biotin), 1.75–1.28 ppm (m, 6H; $COCH_2(CH_2)_3$ biotin); IR (KBr): $\tilde{\nu}=3280$ (N–H), 1709 (C=O), 1636 cm^{-1} (C=O); positive-ion ESI-MS ion clusters at *m*/*z* [M^+]: 545 [dpqB+H]$^+$.

DppzB: A solution of CDI (178 mg, 1.10 mmol) in DMF (5 mL) was added to a suspension of dppz-COOH (73 mg, 0.22 mmol) in DMF (45 mL). The mixture was heated at 80 °C under nitrogen until the grey solid was dissolved. Then, biotin-en (63 mg, 0.22 mmol) in DMF (5 mL) was added to the brown solution. The solution was heated at 80 °C under nitrogen for 16 h and was then evaporated to dryness under vacuum. The brown solid was washed with chloroform and diethyl ether. Subsequent recrystallization of the product from a MeOH/diethyl ether mixture gave a brown solid (100 mg, 75%). ^{1}H NMR (300 MHz, CD_3OD, 298 K, TMS): $\delta=9.74$–9.70 (m, 2H; H_c, H_g), 9.21–9.19 (m, 2H; H_a, H_i), 8.97 (d, $J=0.6$ Hz, 1H; H_d), 8.51–8.47 (m, 1H; H_f), 8.41–8.38 (m, 1H; H_e), 7.98–7.91 (m, 2H; H_b, H_h), 4.51–4.47 (m, 1H; NCH biotin), 4.32–4.28 (m, 1H; NCH biotin), 3.53–3.43 (m, 4H; NH(CH_2)$_2$NH), 3.07–3.06 (m, 1H; SCH biotin), 2.93 (dd, $J=12.6$, 5.0 Hz, 1H; SCH biotin), 2.70 (d, $J=12.6$ Hz, 1H; SCH biotin), 2.32–2.15 (m, 2H; COCH_2 biotin), 1.66–1.43 ppm (m, 6H; $COCH_2(CH_2)_3$ biotin); IR (KBr): $\tilde{\nu}=3278$ (N–H), 1701 (C=O), 1647 cm^{-1} (C=O); positive-ion ESI-MS clusters at *m*/*z* [M^+]: 596 [dppzB+H]$^+$.

[Ir(ppy)$_2$(dpq)](PF$_6$) (1): A mixture of $[Ir_2(ppy)_4Cl_2]$ (68 mg, 0.06 mmol) and dpq (29 mg, 0.12 mmol) in MeOH/CH_2Cl_2 (40 mL, 1:1) was heated under reflux under an inert atmosphere of nitrogen in the dark for 4 h. The orange solution was then cooled to room temperature and KPF_6 (26 mg, 0.14 mmol) was added to the solution. The mixture was then evaporated to dryness and the solid was dissolved in CH_2Cl_2 and purified by column chromatography on silica gel. The desired product was eluted with CH_2Cl_2/acetone (9:1). Subsequent recrystallization of the complex from a CH_2Cl_2/diethyl ether mixture afforded complex **1** as yellow crystals (83 mg, 73%). ^{1}H NMR (300 MHz, [D$_6$]acetone, 298 K, TMS): $\delta=9.78$ (dd, $J=8.5$, 1.8 Hz, 2H; H_c dpq), 9.35 (s, 2H; H_d dpq), 8.56 (dd, $J=5.3$, 1.5 Hz, 2H; H_a dpq), 8.27–8.18 (m, 4H; H3 pyridyl ring ppy$^-$, H_b dpq), 7.97–7.89 (m, 4H; H3 phenyl ring, H4 pyridyl ring ppy$^-$), 7.82–7.80 (td, $J=5.3$, 0.8 Hz, 2H; H6 pyridyl ring ppy$^-$), 7.13–7.06 (dt, $J=7.3$, 1.2 Hz, 2H; H4 phenyl ring ppy$^-$), 7.01–6.96 (m, 4H; H5 phenyl ring, H5 pyridyl ring ppy$^-$), 6.46 ppm (dd, $J=7.6$, 0.9 Hz, 2H; H6 phenyl ring ppy$^-$); IR (KBr): $\tilde{\nu}=840$ cm^{-1} (PF_6^-); positive-ion ESI-MS ion clusters at *m*/*z* [M^+]: 732 [Ir(ppy)$_2$(dpq)]$^+$; elemental analysis calcd (%) for $C_{36}H_{24}N_6F_6PIr\cdot H_2O$: C 48.27, H 2.93, N 9.38; found: C 48.21, H 3.21, N 9.61.

[Ir(ppy)$_2$(dpqa)](PF$_6$) (2): The procedure was similar to that described for the preparation of complex **1**, except that dpqa (42 mg, 0.12 mmol) was used instead of dpq. Complex **2** was isolated as yellow crystals (100 mg, 81%). ^{1}H NMR (300 MHz, [D$_6$]acetone, 298 K, TMS): $\delta=10.03$ (dd, $J=8.5$, 1.5 Hz, 1H; H_c dpqa), 9.85 (s, 1H; H_d dpqa), 9.80 (dd, $J=8.5$, 1.5 Hz, 1H; H_e dpqa), 9.16 (t, $J=6.5$ Hz, 1H; N–H), 8.60–8.55 (m, 2H; H_a, H_g dpqa), 8.30–8.21 (m, 4H; H3 pyridyl ring ppy$^-$, H_b, H_f dpqa), 7.97–7.89 (m, 4H; H3 phenyl ring, H4 pyridyl ring ppy$^-$), 7.83 (d, $J=5.9$ Hz, 1H; H6 pyridyl ring ppy$^-$), 7.78 (dd, $J=5.0$ Hz, 1H; H6 pyridyl ring ppy$^-$), 7.10 (dt, $J=7.6$, 1.5 Hz, 2H; H4 pyridyl ring ppy$^-$), 7.02–6.96 (m, 4H; H5 phenyl ring, H5 pyridyl ring ppy$^-$), 6.46 (d, $J=7.0$ Hz, 2H; H6 phenyl ring ppy$^-$), 3.60–3.52 (m, 2H; CH_2(CH$_2$)$_2$CH$_3$), 1.73–1.64 (m, 2H; CH$_2$CH_2CH$_2$CH$_3$), 1.50–1.38 (m, 2H; (CH$_2$)$_2$CH_2CH$_3$), 0.96 ppm (t, $J=7.3$ Hz, 3H; CH$_3$); IR (KBr): $\tilde{\nu}=3498$ (N–H), 3396 (N–H), 1671 (C=O), 846 cm^{-1} (PF_6^-); positive-ion ESI-MS ion-cluster at *m*/*z* [M^+]: 832 [Ir(ppy)$_2$(dpqa)]$^+$, 501 [Ir(ppy)$_2$]$^+$; elemental analysis calcd (%) for $C_{41}H_{33}N_7OF_6PIr\cdot 1.5H_2O$: C 49.05, H 3.61, N 9.77; found: C 49.23, H 3.80, N 9.54.

[Ir(ppy)$_2$(dpqB)](PF$_6$) (3): The procedure was similar to that described for the preparation of complex **1**, except that dpqB (74 mg, 0.12 mmol) was used instead of dpq and that the reactants were heated under reflux in a mixture of MeOH/CH_2Cl_2 (3:1) and MeOH was used to elute the product from an alumina column. Complex **3** was isolated as orange crystals (75 mg, 46%). ^{1}H NMR (300 MHz, [D$_6$]acetone, 298 K, TMS): $\delta=10.39$ (dt, $J=7.5$, 1.5 Hz, 1H; H_c dpqB), 9.80–9.71 (m, 3H; H_d, H_e dpqB, dpqB-CONH), 8.59–8.56 (m, 2H; H_a, H_g dpqB), 8.31–8.22 (m, 4H; H3 pyridyl ring ppy$^-$, H_b, H_f dpqB), 7.97–7.78 (m, 7H; H3 phenyl ring, H4, H6 pyridyl ring ppy$^-$, NH(CH$_2$)$_2$N*H*CO), 7.10 (t, $J=7.6$ Hz, 2H; H4 phenyl ring ppy$^-$), 7.02–6.96 (m, 4H; H5 phenyl ring, H5 pyridyl ring ppy$^-$), 6.45 (td, $J=7.3$, 1.2 Hz, 2H; H6 phenyl ring ppy$^-$), 5.55–5.44 (m, 2H; N–H biotin), 4.35–4.21 (m, 1H; NCH biotin), 4.10–4.02 (m, 1H; NCH biotin), 3.65–3.54 (m, 4H; NH(CH_2)$_2$NH), 2.95–2.84 (m, 1H; SC*H*-(CH$_2$)$_4$) biotin), 2.67–2.60 (m, 1H; SCH biotin), 2.47–2.41 (m, 1H; SCH biotin), 2.33–2.24 (m, 2H; COCH_2 biotin), 1.67–1.27 ppm (m, 6H; $COCH_2(CH_2)_3$ biotin); IR (KBr): $\tilde{\nu}=3423$ (N–H), 3268 (N–H), 1676 (C=O), 844 cm^{-1} (PF_6^-); positive-ion ESI-MS ion clusters at *m*/*z* [M^+]: 1045 [Ir(ppy)$_2$(dpqB)]$^+$, 501 [Ir(ppy)$_2$]$^+$; elemental analysis calcd (%) for $C_{49}H_{44}N_{10}O_3SF_6PIr\cdot 3H_2O$: C 47.30, H 4.05, N 11.26; found: C 47.34, H 4.11, N 11.41.

[Ir(ppy)$_2$(dppz)](PF$_6$) (4): The procedure was similar to that described for the preparation of complex **1**, except that dppz (36 mg, 0.12 mmol) was used instead of dpq. Complex **4** was isolated as orange crystals (62 mg, 37%). ^{1}H NMR (300 MHz, [D$_6$]acetone, 298 K, TMS): $\delta=9.89$ (dd, $J=8.2$, 1.5 Hz, 2H; H_c dppz), 8.56–8.51 (m, 4H; H_a, H_d dppz), 8.29–8.20 (m, 6H; H3 pyridyl ring ppy$^-$, H_b, H_e dppz), 7.98–7.87 (m, 6H; H4, H6 pyridyl ring, H3 phenyl ring ppy$^-$), 7.11 (dt, $J=7.6$, 1.2 Hz, 2H; H4 phenyl ring ppy$^-$), 7.05–6.97 (m, 4H; H5 pyridyl ring, H5 phenyl ring ppy$^-$), 6.47 ppm (dd, $J=7.3$, 0.9 Hz, 2H; H6 phenyl ring ppy$^-$); IR (KBr): $\tilde{\nu}=839$ cm^{-1} (PF^-); positive-ion ESI-MS ion clusters at *m*/*z* [M^+]: 782 [Ir(ppy)$_2$(dppz)]$^+$, 501 [Ir(ppy)$_2$]$^+$; elemental analysis calcd (%) for $C_{40}H_{26}N_6F_6PIr\cdot 0.5H_2O$: C 51.28, H 2.90, N 8.97; found: C 51.24, H 3.05, N 8.83.

[Ir(ppy)$_2$(dppn)](PF$_6$) (5): The procedure was similar to that described for the preparation of complex **1**, except that dppn (42 mg, 0.12 mmol) was used instead of dpq. Complex **5** was isolated as orange crystals (41 mg, 33%). ^{1}H NMR (300 MHz, [D$_6$]acetone, 298 K, TMS): $\delta=9.89$ (dd, $J=8.1$, 1.2 Hz, 2H; H_c dppn), 9.21 (s, 2H; H_d dppn), 8.53 (dd, $J=5.3$, 1.5 Hz, 2H; H_a dppn), 8.44 (dd, $J=6.6$, 3.5 Hz, 2H; H_b dppn), 8.31–8.22 (m, 4H; H3 pyridyl ring ppy$^-$, H_e dppn), 7.99–7.92 (m, 6H; H4, H6 pyridyl ring, H3 phenyl ring ppy$^-$), 7.81 (dd, $J=6.6$, 2.9 Hz, 2H; H_f dppn), 7.13–6.98 (m, 6H; H5 pyridyl ring, H4, H5 phenyl ring ppy$^-$), 6.47 ppm (d, $J=7.3$ Hz, 2H; H6 phenyl ring ppy$^-$); IR (KBr): $\tilde{\nu}=844$ cm^{-1} (PF^-); positive-ion ESI-MS ion clusters at *m*/*z* [M^+]: 832 [Ir(ppy)$_2$(dppn)]$^+$, 501 [Ir(ppy)$_2$]$^+$; elemental analysis calcd (%) for $C_{44}H_{28}N_6F_6PIr\cdot H_2O$: C 53.06, H 3.04, N 8.44; found: C 52.87, H 3.05, N 8.40.

[Ir(ppy)$_2$(dppzB)](PF$_6$) (6): The procedure was similar to that described for the preparation of complex **1**, except that dppzB (77 mg, 0.12 mmol)

was used instead of dpq and that the reactants were refluxed in a mixture of MeOH/CH_2Cl_2 (5:1) and a solvent mixture of CH_3CN/MeOH (9:1) was used to elute the product from an alumina column. Complex **6** was isolated as orange crystals (123 mg, 30%). ^{1}H NMR (300 MHz, [D_6]acetone, 298 K, TMS): δ = 9.92–9.87 (m, 2H; H_c, H_g dppzB), 8.96 (s, 1H; H_e dppzB), 8.68 (s, 1H; dppz-CONH), 8.56–8.55 (m, 4H; H_a, H_d, H_f, H_i dppzB), 8.30–8.23 (m, 4H; H3 pyridyl ring ppy$^-$, H_b, H_h dppzB), 7.98–7.88 (m, 6H; H3 phenyl ring, H4, H6 pyridyl ring ppy$^-$), 7.65 (s, 1H; $NH(CH_2)_2NHCO$), 7.14–6.97 (m, 6H; H4, H5 phenyl ring, H5 pyridyl ring ppy$^-$), 6.46 (d, J = 7.3 Hz, 2H; H6 phenyl ring ppy$^-$), 5.64 (s, 1H; NH biotin), 5.54 (s, 1H; NH biotin), 4.38–4.36 (m, 1H; NCH biotin), 4.23–4.19 (m, 1H; NCH biotin), 3.62–3.59 (m, 4H; $NH(CH_2)_2NH$), 2.60–2.53 (m, 2H; SCH_2 biotin), 2.28–2.24 (m, 2H; $COCH_2$ biotin), 1.67–1.41 ppm (m, 6H; $COCH_2(CH_2)_3$ biotin); IR (KBr): $\tilde{\nu}$ = 3415 (N–H), 1694 (C=O), 1653 (C=O), 844 cm^{-1} (s, PF^-); positive-ion ESI-MS ion-clusters at m/z [M^+]: 1094 [Ir(ppy)$_2$(dppzB)]$^+$, 501 [Ir(ppy)$_2$]$^+$; elemental analysis calcd (%) for $C_{53}H_{46}N_{10}O_3SF_6PIr\cdot 2H_2O$: C 49.88, H 3.95, N 10.97; found: C 49.59, H 4.13, N 10.69. Reversed-phase HPLC analysis: Alltima C18 column (53 × 7 mm, 3 μm), isocratic 95% aqueous MeOH, flow rate = 1 mL min^{-1}, t_R = 1.40 min.

DNA absorption and emission titrations: In a typical experiment, aliquots (5 μL) of calf thymus DNA or synthetic oligonucleotides (3.4 mM) in Tris-Cl buffer (50 mM, pH 7.4) were added cumulatively to the iridium complex (84.7 μM) in a mixture of the same buffer and methanol (7:3) at 1 min intervals. The absorption and emission spectra of the solution were measured. For solubility reasons, the trifluoromethanesulfonate salts of complexes **4** and **5** were used while the hexafluorophosphate salts of other complexes were employed. Although these complexes were only sparingly soluble in pure aqueous solutions, addition of aqueous buffer to a methanolic solution of the complexes to give a buffer/methanol (7:3) mixture did not cause any precipitation problems. The solutions remained visually clear, the baselines of the absorption spectra of all the complexes in this solvent mixture did not increase, and no scattering effects were observed in the measured emission spectra.

HABA assays: In a typical experiment, aliquots (5 μL) of complex **3** or **6** (550 μM) in methanol were added cumulatively to a mixture of avidin (3.8 μM) and HABA (0.3 mM) in potassium phosphate buffer (2 mL, 50 mM, pH 7.4) at 1 min intervals. The binding of the complexes to avidin was indicated by the decrease of absorbance at 500 nm due to the displacement of HABA from the avidin by the complexes. The binding stoichiometries of the complexes to avidin were determined from a plot of $-\Delta A_{500\,nm}$ versus [Ir]:[avidin].

Determination of k_{on}, k_{off}, and K_d: The K_d value is defined as the ratio k_{off}/k_{on}, where k_{on} is the bimolecular rate constant for the binding of the fourth iridium(III)–biotin complex to avidin–Ir_3, and k_{off} is the unimolecular rate constant for the dissociation of the first iridium(III)–biotin complex from the fully bound adduct avidin–Ir_4 (as induced by addition of excess unmodified biotin molecules).[43] In the association studies, an avidin solution was added to four equivalents of complex **3** or **6** in an emission cuvette. The emission intensity of the solution was measured. The on-rate constant k_{on} for the binding of the complexes to avidin was estimated from Equation (3):[43]

$$\frac{1}{F-F_4'} = \frac{1}{F_3'-F_4'} + \frac{1}{F_3'-F_4'}(a/V)k_{on}t \quad (3)$$

where F = emission intensity at time = t, F_3' = initial emission intensity, F_4' = final emission intensity, a = number of moles of avidin added, V = total volume of solution, t = reaction time after avidin was added.

In practice, F_4' was varied until the plot of $1/(F-F_4')$ against t was linear. The y intercept and slope of the linear-fit gave $1/(F_3'-F_4')$ and $(F_3'-F_4')^{-1}(a/V)k_{on}$, respectively. Thus, the constant k_{on} can be determined.

The dissociation of the iridium(III)–biotin complex from avidin was induced by addition of an excess of unmodified biotin. The subsequent decrease in emission intensity was interpreted in terms of a monomolecular reaction. The off-rate constant k_{off} was determined according to Equation (4):[43]

$$\frac{F-F_3}{F_4-F_3} = -k_{off}t \quad (4)$$

where F_4 = initial emission intensity of the iridium(III)–avidin adduct, F_3 = emission intensity after dissociation of one equivalent of iridium(III)-biotin, t = reaction time after excess biotin was added.

The slope of the linear fit of $(F-F_3)/(F_4-F_3)$ against t gave the constant $-k_{off}$.

X-ray structure analysis for complex 4: Single crystals of the complex suitable for X-ray crystallographic studies were obtained by layering of petroleum ether (b.p. 40–60 °C) over a concentrated acetone solution of the complex. A crystal of dimensions 0.2 × 0.15 × 0.1 mm^3 mounted in a glass capillary was used for data collection at −20 °C on a MAR diffractometer with a 300 mm image-plate detector by using graphite monochromatized $Mo_{K\alpha}$ radiation (λ = 0.710 73 Å). Data collection was made with 2° oscillation steps of ϕ, 600 s exposure time, and a scanner distance at 120 mm. A total of 100 images were collected. The images were interpreted and intensities integrated using the program DENZO.[49] The structure was solved by direct methods employing the program SHELXS-97[50] on a PC. Iridium, phosphorus, and many nonhydrogen atoms were located according to the direct methods. The positions of other nonhydrogen atoms were found after successful refinement by full-matrix least-squares by using the program SHELXL-97.[50] Two individual molecules were located in the asymmetric unit together with one acetone and two water oxygen atoms. One crystallographic asymmetric unit consisted of two formula units. In the final stage of least-squares refinement, the iridium atoms were refined anisotropically and other atoms isotropi-

Table 7. Crystal data and summary of data collection and refinement for complex **4**.

formula	$C_{41.50}H_{31}F_6IrN_6O_{1.50}P$
M_w	974.89
crystal size [mm^3]	0.2 × 0.15 × 0.1
T [K]	253(2)
crystal system	triclinic
space group	$P\bar{1}$ (no. 2)
a [Å]	13.908(3)
b [Å]	16.322(3)
c [Å]	20.112(4)
α [°]	93.93(3)
β [°]	98.92(3)
γ [°]	94.50(3)
V [Å^3]	4481.3(16)
Z	4
ρ_{calcd} [mg m^{-3}]	1.445
μ [mm^{-1}]	3.078
F(000)	1920
θ range [°]	1.49–22.63
oscillations [°]	2
no. images collected	100
distance [mm]	120
exposure time [s]	600
index ranges	$-12 \le h \le 12$ $-15 \le k \le 16$ $-19 \le l \le 20$
no. data collected	12211
R_{int}[a]	0.0795
no. of unique data/restraints/parameters	6611/5/491
GOF on F^2[b]	0.914
R_1, wR_2 ($I > 2\sigma(I)$)[c]	0.0783, 0.1942
R_1, wR_2 (all data)	0.1576, 0.2393
largest diff. peak/hole [e Å^{-3}]	1.050, −0.747

[a] $R_{int} = \Sigma|F_o^2 - F_c^2(\text{mean})|/\Sigma[F_o^2]$. [b] GOF = $\{\Sigma[w(F_o^2-F_c^2)^2]/(n-p)\}^{1/2}$, where n is the number of reflections and p is the total number of parameters refined. The weighting scheme is $w = 1/[\sigma^2(F_o^2) + (aP)^2 + bP]$, where $P = [2F_o^2 + \max(F_o^2, 0)]/3$, a = 0.1112 and b = 0.0000. [c] $R_1 = \Sigma||F_o| - |F_c||/\Sigma|F_o|$, $wR_2 = \{\Sigma[w(F_o^2-F_c^2)^2]/\Sigma[w(F_o^2)^2]\}^{1/2}$.

cally. Hydrogen atoms were generated by the program SHELXL-97. The positions of the hydrogen atoms (except those on acetone and water oxygen) were calculated based on the riding mode with thermal parameters equal to 1.2-times that of the associated carbon atoms, and were used in the calculation of final *R* indices. Crystal data and a summary of data collection and refinement details are given in Table 7.

CCDC-218619 contains the supplementary crystallographic data for this paper. These data can be obtained free of charge from the Cambridge Crystallographic Data Centre via www.ccdc.cam.ac.uk/data_request/cif/.

Acknowledgements

We thank the Hong Kong Research Grants Council (Project Nos. CityU 101603 and CityU 1113/02P) and City University of Hong Kong (Project No. 7001456) for financial support. C.K.C. acknowledges the receipt of a Postgraduate Studentship and a Research Tuition Scholarship, both administered by the City University of Hong Kong. We also thank the Faculty of Science and Engineering of the City University of Hong Kong for support (Project No. 9610020).

[1] See, for example: a) K. W. Jennette, S. J. Lippard, G. A. Vassiliades, W. R. Bauer, *Proc. Natl. Acad. Sci. USA* **1974**, *71*, 3839; b) S. J. Lippard, *Acc. Chem. Res.* **1978**, *11*, 211; c) Metal-DNA Chemistry in *ACS Symposium Series 402* (Ed.: T. D. Tullis), American Chemical Society, Washington D.C., **1989**; d) D. S. Sigma, A. Mazumder, D. M. Perrin, *Chem. Rev.* **1993**, *93*, 2295; e) B. Nordén, P. Lincoln, B. Åkerman, E. Tuite in *Metal Ions in Biological Systems, Vol. 33* (Eds.: A. Sigel, H. Sigel), Marcel Dekker, New York, **1996**, p. 177; f) K. E. Erkkila, D. T. Odom, J. K. Barton, *Chem. Rev.* **1999**, *99*, 2777; g) C. Metcalfe, J. A. Thomas, *Chem. Soc. Rev.* **2003**, *32*, 215.

[2] a) I. Greguric, J. R. Aldrich-Wright, J. G. Collins, *J. Am. Chem. Soc.* **1997**, *119*, 3621; b) J. G. Collins, A. D. Sleeman, J. R. Aldrich-Wright, I. Greguric, T. W. Hambley, *Inorg. Chem.* **1998**, *37*, 3133; c) J. G. Collins, J. R. Aldrich-Wright, I. D. Greguric, P. Pellegrini, *Inorg. Chem.* **1999**, *38*, 5502.

[3] a) K. A. O'Donoghue, J. M. Kelly, P. E. Kruger, *Dalton Trans.* **2004**, 13; b) K. A. O'Donoghue, J. C. Penedo, J. M. Kelly, P. E. Kruger, *Dalton Trans.* **2005**, 1123.

[4] a) R. M. Hartshorn, J. K. Barton, *J. Am. Chem. Soc.* **1992**, *114*, 5919; b) Y. Jenkins, J. K. Barton, *J. Am. Chem. Soc.* **1992**, *114*, 8736; c) C. J. Murphy, M. R. Arkin, Y. Jenkins, N. D. Ghatlia, S. H. Bossmann, R. E. Holmlin, J. K. Barton, *Science* **1993**, *262*, 1025; d) M. R. Arkin, E. D. A. Stemp, R. E. Holmlin, J. K. Barton, A. Hörmann, E. J. C. Olson, P. F. Barbara, *Science* **1996**, *273*, 475; e) R. E. Holmlin, J. A. Yao, J. K. Barton, *Inorg. Chem.* **1999**, *38*, 174; f) C. Stinner, M. D. Wightman, S. O. Kelley, M. G. Hill, J. K. Barton, *Inorg. Chem.* **2001**, *40*, 5245; g) S. Delaney, M. Pascaly, P. K. Bhattacharya, K. Han, J. K. Barton, *Inorg. Chem.* **2002**, *41*, 1966.

[5] a) C. Hiort, P. Lincoln, B. Nordén, *J. Am. Chem. Soc.* **1993**, *115*, 3448; b) I. Haq, P. Lincoln, D. Suh, B. Nordén, B. Z. Chowdhry, J. B. Chaires, *J. Am. Chem. Soc.* **1995**, *117*, 4788; c) P. Lincoln, A. Broo, B. Nordén, *J. Am. Chem. Soc.* **1996**, *118*, 2644; d) C. G. Coates, J. Olofsson, M. Coletti, J. J. McGarvey, B. Önfelt, P. Lincoln, B. Nordén, E. Tuite, P. Matousek, A. W. Parker, *J. Phys. Chem. B* **2001**, *105*, 12653; e) B. H. Yun, J. O. Kim, B. W. Lee, P. Lincoln, B. Nordén, J.-M. Kim, S. K. Kim, *J. Phys. Chem. B* **2003**, *107*, 9858.

[6] a) N. Gupta, N. Grover, G. A. Neyhart, W. Liang, P. Singh, H. H. Thorp, *Angew. Chem.* **1992**, *104*, 1058; *Angew. Chem. Int. Ed. Engl.* **1992**, *31*, 1048; b) W. A. Kalsbeck, H. H. Thorp, *J. Am. Chem. Soc.* **1993**, *115*, 7146; c) S. R. Smith, G. A. Neyhart, W. A. Kalsbeck, H. H. Thorp, *New J. Chem.* **1994**, *18*, 397.

[7] H. D. Stoeffler, N. B. Thornton, S. L. Temkin, K. S. Schanze, *J. Am. Chem. Soc.* **1995**, *117*, 7119.

[8] a) C. Metcalfe, M. Webb, J. A. Thomas, *Chem. Commun.* **2002**, 2026; b) C. Metcalfe, H. Adams, I. Haq, J. A. Thomas, *Chem. Commun.* **2003**, 1152.

[9] a) V. W.-W. Yam, K. K.-W. Lo, K.-K. Cheung, R. Y.-C. Kong, *J. Chem. Soc. Chem. Commun.* **1995**, 1191; b) V. W.-W. Yam, K. K.-W. Lo, K.-K. Cheung, R. Y.-C. Kong, *J. Chem. Soc. Dalton Trans.* **1997**, 2067.

[10] K. K.-W. Lo, K. H.-K. Tsang, *Organometallics* **2004**, *23*, 3062.

[11] K. D. Barker, B. R. Benoit, J. A. Bordelon, R. J. Davis, A. S. Delmas, O. V. Mytykh, J. T. Petty, J. F. Wheeler, N. A. P. Kane-Maguire, *Inorg. Chim. Acta* **2001**, *322*, 74.

[12] S. Arounaguiri, B. G. Maiya, *Inorg. Chem.* **1996**, *35*, 4267.

[13] a) D. Herebian, W. S. Sheldrick, *J. Chem. Soc. Dalton Trans.* **2002**, 966; b) A. Frodl, D. Herebian, W. S. Sheldrick, *J. Chem. Soc. Dalton Trans.* **2002**, 3664.

[14] M. S. Lowry, W. R. Hudson, R. A. Pascal, Jr., S. Bernhard, *J. Am. Chem. Soc.* **2004**, *126*, 14129.

[15] a) Y. Ohsawa, S. Sprouse, K. A. King, M. K. DeArmond, K. W. Hanck, R. J. Watts, *J. Phys. Chem.* **1987**, *91*, 1047; b) F. O. Garces, K. A. King, R. J. Watts, *Inorg. Chem.* **1988**, *27*, 3464; c) A. P. Wilde, R. J. Watts, *J. Phys. Chem.* **1991**, *95*, 622; d) A. P. Wilde, K. A. King, R. J. Watts, *J. Phys. Chem.* **1991**, *95*, 629.

[16] a) S. Serroni, A. Juris, S. Campagna, M. Venturi, G. Denti, V. Balzani, *J. Am. Chem. Soc.* **1994**, *116*, 9086; b) G. Calogero, G. Giuffrida, S. Serroni, V. Ricevuto, S. Campagna, *Inorg. Chem.* **1995**, *34*, 541; c) F. Neve, A. Crispini, S. Campagna, S. Serroni, *Inorg. Chem.* **1999**, *38*, 2250; d) P. M. Griffiths, F. Loiseau, F. Puntoriero, S. Serroni, S. Campagna, *Chem. Commun.* **2000**, 2297; e) F. Neve, M. La Deda, A. Crispini, A. Bellusci, F. Puntoriero, S. Campagna, *Organometallics* **2004**, *23*, 5856.

[17] a) M. Polson, S. Fracasso, V. Bertolasi, M. Ravaglia, F. Scandola, *Inorg. Chem.* **2004**, *43*, 1950; b) M. Polson, M. Ravaglia, S. Fracasso, M. Garavelli, F. Scandola, *Inorg. Chem.* **2005**, *44*, 1282.

[18] a) P. Didier, I. Ortmans, A. Kirsch-De Mesmaeker, R. J. Watts, *Inorg. Chem.* **1993**, *32*, 5239; b) I. Ortmans, P. Didier, A. Kirsch-De Mesmaeker, *Inorg. Chem.* **1995**, *34*, 3695.

[19] a) J.-P. Collin, I. M. Dixon, J.-P. Sauvage, J. A. G. Williams, F. Barigelletti, L. Flamigni, *J. Am. Chem. Soc.* **1999**, *121*, 5009; b) I. M. Dixon, J.-P. Collin, J.-P. Sauvage, L. Flamigni, S. Encinas, F. Barigelletti, *Chem. Soc. Rev.* **2000**, *29*, 385; c) I. M. Dixon, J.-P. Collin, J.-P. Sauvage, F. Barigelletti, L. Flamigni, *Angew. Chem.* **2000**, *112*, 1348; *Angew. Chem. Int. Ed.* **2000**, *39*, 1292; d) L. Flamigni, I. M. Dixon, J.-P. Collin, J.-P. Sauvage, *Chem. Commun.* **2000**, 2479; e) E. Baranoff, I. M. Dixon, J.-P. Collin, J.-P. Sauvage, B. Ventura, L. Flamigni, *Inorg. Chem.* **2004**, *43*, 3057; f) L. Flamigni, B. Ventura, F. Barigelletti, E. Baranoff, J.-P. Collin, J.-P. Sauvage, *Eur. J. Inorg. Chem.* **2005**, 1312.

[20] a) M. G. Colombo, H. U. Güdel, *Inorg. Chem.* **1993**, *32*, 3081; b) M. G. Colombo, A. Hauser, H. U. Güdel, *Inorg. Chem.* **1993**, *32*, 3088; c) M. G. Colombo, T. C. Brunold, T. Riedener, H. U. Güdel, M. Förtsch, H.-B. Bürgi, *Inorg. Chem.* **1994**, *33*, 545; d) M. G. Colombo, A. Hauser, H. U. Güdel, *Top. Curr. Chem.* **1994**, *171*, 143.

[21] a) S. Lamansky, P. Djurovich, D. Murphy, F. Abdel-Razzaq, H.-E. Lee, C. Adachi, P. E. Burrows, S. R. Forrest, M. E. Thompson, *J. Am. Chem. Soc.* **2001**, *123*, 4304; b) R. Gao, D. G. Ho, B. Hernandez, M. Selke, D. Murphy, P. I. Djurovich, M. E. Thompson, *J. Am. Chem. Soc.* **2002**, *124*, 14828; c) A. B. Tamayo, B. D. Alleyne, P. I. Djurovich, S. Lamansky, I. Tsyba, N. N. Ho, R. Bau, M. E. Thompson, *J. Am. Chem. Soc.* **2003**, *125*, 7377; d) J. Li, P. I. Djurovich, B. D. Alleyne, I. Tsyba, N. N. Ho, R. Bau, M. E. Thompson, *Polyhedron* **2004**, *23*, 419; e) J. Li, P. I. Djurovich, B. D. Alleyne, M. Yousufuddin, N. N. Ho, J. C. Thomas, J. C. Peters, R. Bau, M. E. Thompson, *Inorg. Chem.* **2005**, *44*, 1713.

[22] a) M. Licini, J. A. G. Williams, *Chem. Commun.* **1999**, 1943; b) W. Goodall, J. A. G. Williams, *J. Chem. Soc. Dalton Trans.* **2000**, 2893; c) A. J. Wilkinson, A. E. Goeta, C. E. Foster, J. A. G. Williams, *Inorg. Chem.* **2004**, *43*, 6513; d) W. Leslie, A. S. Batsanov, J. A. K. Howard, J. A. G. Williams, *Dalton Trans.* **2004**, 623; e) W. Leslie, R. A. Poole, P. R. Murray, L. J. Yellowlees, A. Beeby, J. A. G. Williams, *Polyhedron* **2004**, *23*, 2769.

[23] N. P. Ayala, C. M. Flynn, L. Sacksteder, J. N. Demas, B. A. DeGraff, *J. Am. Chem. Soc.* **1990**, *112*, 3837.

[24] a) J. H. van Diemen, J. G. Haasnoot, R. Hage, E. Müller, J. Reedijk, *Inorg. Chim. Acta* **1991**, *181*, 245; b) J. H. van Diemen, R. Hage, J. G. Haasnoot, H. E. B. Lempers, J. Reedijk, J. G. Vos, L. De Cola, F. Barigelletti, V. Balzani, *Inorg. Chem.* **1992**, *31*, 3518.
[25] a) E. A. Plummer, J. W. Hofstraat, L. De Cola, *Dalton Trans.* **2003**, 2080; b) P. Coppo, E. A. Plummer, L. De Cola, *Chem. Commun.* **2004**, 1774; c) P. Coppo, M. Duati, V. N. Kozhevnikov, J. W. Hofstraat, L. De Cola, *Angew. Chem.* **2005**, *117*, 1840; *Angew. Chem. Int. Ed.* **2005**, *44*, 1806.
[26] a) M. Maestri, V. Balzani, C. Deuschel-Cornioley, A. von Zelewsky, *Adv. Photochem.* **1992**, *17*, 1; b) C. Schaffner-Hamann, A. von Zelewsky, A. Barbieri, F. Barigelletti, G. Muller, J. P. Riehl, A. Neels, *J. Am. Chem. Soc.* **2004**, *126*, 9339.
[27] T. Yutaka, S. Obara, S. Ogawa, K. Nozaki, N. Ikeda, T. Ohno, Y. Ishii, K. Sakai, M. Haga, *Inorg. Chem.* **2005**, *44*, 4737.
[28] a) F.-M. Hwang, H.-Y. Chen, P.-S. Chen, C.-S. Liu, Y. Chi, C.-F. Shu, F.-L. Wu, P.-T. Chou, S.-M. Peng, G.-H. Lee, *Inorg. Chem.* **2005**, *44*, 1344; b) H.-C. Li, P.-T. Chou, Y.-H. Hu, Y.-M. Cheng, R.-S. Liu, *Organometallics* **2005**, *24*, 1329.
[29] a) E. Holder, V. Marin, M. A. R. Meier, U. S. Schubert, *Macromol. Rapid Commun.* **2004**, *25*, 1491; b) E. Holder, V. Marin, A. Alexeev, U. S. Schubert, *J. Polym. Sci. Pol. Chem.* **2005**, *43*, 2765.
[30] a) K. K.-W. Lo, D. C. M. Ng, C. K. Chung, *Organometallics* **2001**, *20*, 4999; b) K. K.-W. Lo, C.-K. Chung, D. C.-M. Ng, N. Zhu, *New J. Chem.* **2002**, *26*, 81; c) K. K.-W. Lo, C.-K. Chung, N. Zhu, *Chem. Eur. J.* **2003**, *9*, 475; d) K. K.-W. Lo, C.-K. Chung, T. K.-M. Lee, L.-H. Lui, K. H.-K. Tsang, N. Zhu, *Inorg. Chem.* **2003**, *42*, 6886; e) K. K.-W. Lo, J. S.-W. Chan, L.-H. Lui, C.-K. Chung, *Organometallics* **2004**, *23*, 3108; f) K. K.-W. Lo, J. S.-W. Chan, C.-K. Chung, V. W.-H. Tsang, N. Zhu, *Inorg. Chim. Acta* **2004**, *357*, 3109; g) K. K.-W. Lo, C.-K. Li, J. S.-Y. Lau, *Organometallics* **2005**, *24*, 4594.
[31] A. Delgadillo, P. Romo, A. M. Leiva, B. Loeb, *Helv. Chim. Acta* **2003**, *86*, 2110.
[32] J. E. Dickeson, L. A. Summers, *Aust. J. Chem.* **1970**, *23*, 1023.
[33] M. Wilchek, E. A. Bayer, *Methods Enzymol.* **1990**, *184*, 123.
[34] D. Ossipov, E. Zamaratski, J. Chattopadhyaya, *Helv. Chim. Acta* **1999**, *82*, 2186.
[35] R. K. Garlick, R. W. Giese, *J. Biol. Chem.* **1988**, *263*, 210.
[36] V. A. Bloomfield, D. M. Crothers, I. J. Tinoco, *Physical Chemistry of Nucleic Acid*, Harper and Row, New York, **1974**.
[37] M. T. Carter, M. Rodriguez, A. J. Bard, *J. Am. Chem. Soc.* **1989**, *111*, 8901.
[38] Due to solubility reasons, the titration experiments were performed in a mixture of Tris-Cl buffer (50 mM, pH 7.4) and methanol (7:3).
[39] J. Marmur, P. Doty, *J. Mol. Biol.* **1962**, *5*, 109.
[40] M. Wilchek, E. A. Bayer, *Anal. Biochem.* **1988**, *171*, 1.
[41] M. Wilchek, E. A. Bayer, *Methods Enzymol., Vol. 184*, Academic Press, San Diego, **1990**.
[42] a) K. K.-W. Lo, W.-K. Hui, D. C.-M. Ng, *J. Am. Chem. Soc.* **2002**, *124*, 9344; b) K. K.-W. Lo, T. K.-M. Lee, *Inorg. Chem.* **2004**, *43*, 5275; c) K. K.-W. Lo, W.-K. Hui, *Inorg. Chem.* **2005**, *44*, 1992.
[43] M. Marek, K. Kaiser, H. J. Gruber, *Bioconjugate Chem.* **1997**, *8*, 560.
[44] D. D. Perrin, W. L. F. Armarego, *Purification of Laboratory Chemicals*, 3rd ed., Pergamon Press, New York, **1988**.
[45] T. Maniatis, E. F. Fritsch, J. Sambrook, *Molecular Cloning: A Laboratory Manual*, Cold Spring Harbor Laboratory, New York, **1982**, p. 458.
[46] C. V. Kumar, E. H. Asuncion, *J. Am. Chem. Soc.* **1993**, *115*, 8547.
[47] J. N. Demas, G. A. Crosby, *J. Phys. Chem.* **1971**, *75*, 991.
[48] K. Nakamaru, *Bull. Chem. Soc. Jpn.* **1982**, *55*, 2697.
[49] Z. Otwinowski, W. Minor, DENZO Program: *Methods Enzymol., Vol. 276*, Academic Press, San Diego, **1997**, p. 307.
[50] G. M. Sheldrick, SHELXS-97 and SHELXL-97, Programs for Crystal Structure Analysis (Release 97-2), University of Göttingen, Göttingen (Germany), **1997**.

Received: July 26, 2005
Published online: November 22, 2005

